Manuscript Details

Manuscript number	COST_2016_668
Title	Flexural Behaviour of Multi-Celled GFRP Composite Beams with Concrete Infill: Experiment and theoretical analysis
Article type	Full Length Article

Abstract

This research introduces multi-celled glass fibre reinforced polymer (GFRP) beam sections partially filled with concrete. Pultruded GFRP square tubes (125 mm x125 mm x 6.5 mm) were bonded together using epoxy adhesives to form the beams using 2 to 4 cells. Concrete with 15 and 32 MPa compressive strengths was used to fill the top cell of the beams. These beams were then tested under static four-point bending and their behaviour was compared with hollow beams. The results showed that up to 27% increase in strength was achieved by multi-celled compared to a single cell beam. The beams with concrete infill failed at 38% to 80% higher load and exhibited 10 to 22% higher stiffness than their hollow counterparts. The increase in the compressive strength of the concrete infill from 15 MPa to 32 MPa resulted in up to 14% increase in the failure load but did not enhance the flexural stiffness. Finally, the proposed prediction equation which account for the combined effect of shear and flexural stresses showed a good agreement with the experimental results for hollow cells and up to 3 cells of concrete filled beams. The bearing stress equation gave a better estimation for 4-cell filled section.

Keywords	Composite beam, multi-cell beams, concrete in-fill, flexural behaviour, theoretical prediction.
Corresponding Author	Allan Manalo
Corresponding Author's Institution	University of Southern Queensland
Order of Authors	Majid Muttashar, Allan Manalo, Warna Karunasena, Weena Lokuge
Suggested reviewers	Yu Bai, Kee Jeung Hong, Takashi Matsumoto

Submission Files Included in this PDF

File Name [File Type]

Manuscript.docx [Manuscript File]

CoverLetter .docx [Cover Letter]

All Figures.pdf [Figure]

All Tables.pdf [Table]

To view all the submission files, including those not included in this PDF, click on the manuscript title on your EVISE Homepage, then click 'Download zip file'.

RESEARCH PAPER

Flexural Behaviour of Multi-Celled GFRP Composite Beams with Concrete Infill: Experiment and theoretical analysis
(Title contains 14 words)

Running headline: Behaviour of Multi-Celled GFRP Composite Beams with Concrete Infill in flexural: Experiment and theoretical analysis
(100 characters)

by

Majid Muttashar[1, 2], Allan Manalo[1], Warna Karunasena[1] and Weena Lokuge[1]
[1] Centre of Excellence in Engineered Fibre Composites (CEEFC),
School of Civil Engineering and Surveying, University of Southern Queensland, Toowoomba 4350, Australia
[2] Department of Civil Engineering, College of Engineering, University of Thi Qar, Iraq.

Submitted to
Composite Structures

Corresponding Author:

Allan Manalo
Senior lecturer in Civil Engineering
Centre of Excellence in Engineered Fibre Composites (CEEFC),
School of Civil Engineering and Surveying,
University of Southern Queensland,
Toowoomba, Queensland 4350, Australia
Tel: (+61) 7 4631 2547 Fax: (+61) 7 4631 2110
E-mail: manalo@usq.edu.au.

Manuscript summary:
Total pages   20 (including cover page)
Number of figures   10
Number of tables   4

0

Flexural Behaviour of Multi-Celled GFRP Composite Beams with Concrete Infill: Experiment and theoretical analysis

Majid Muttashar[1, 2], Allan Manalo[1,*], Warna Karunasena[1] and Weena Lokuge[1]

[1] Centre of Excellence in Engineered Fibre Composites (CEEFC), School of Civil Engineering and Surveying, University of Southern Queensland, Toowoomba 4350, Australia

[2] Department of Civil Engineering, College of Engineering, University of Thi Qar, Iraq.

Email: majid.alzaidy@gmail.com, allan.manalo@usq.edu.au, karu.karunasena@usq.edu.au, weena.lokuge@usq.edu.au

Abstract

This research introduces multi-celled glass fibre reinforced polymer (GFRP) beam sections partially filled with concrete. Pultruded GFRP square tubes (125 mm x125 mm x 6.5 mm) were bonded together using epoxy adhesives to form the beams using 2 to 4 cells. Concrete with 15 and 32 MPa compressive strengths was used to fill the top cell of the beams. These beams were then tested under static four-point bending and their behaviour was compared with hollow beams. The results showed that up to 27% increase in strength was achieved by multi-celled compared to a single cell beam. The beams with concrete infill failed at 38% to 80% higher load and exhibited 10 to 22% higher stiffness than their hollow counterparts. The increase in the compressive strength of the concrete infill from 15 MPa to 32 MPa resulted in up to 14% increase in the failure load but did not enhance the flexural stiffness. Finally, the proposed prediction equation which account for the combined effect of shear and flexural stresses showed a good agreement with the experimental results for hollow cells and up to 3 cells of concrete filled beams. The bearing stress equation gave a better estimation for 4-cell filled section.

Keywords: Composite beam, multi-cell beams, concrete in-fill, flexural behaviour, theoretical prediction.

---

*Corresponding author, tel. (+61) 7 4631 2547; fax. (+61) 7 4631 2110
E-mail addresses: manalo@usq.edu.au (Allan Manalo), majid.alzaidy@gmail.com (Majid Muttashar).

1. Introduction

The corrosion of steel reinforcement is considered the greatest factor limiting the service life of reinforced concrete structures. Thus, innovative and cost-effective materials offering long-term durability and requiring less maintenance, like glass GFRP, are becoming attractive for use in civil engineering applications. Several projects in the construction industry have benefited from the low cost to high-strength of pultruded GFRP thin-walled tubes [1-3]. Despite their many advantageous properties, the relatively low elastic modulus of pultruded GFRP composites resulted in their design governed by serviceability requirements which prevented the full utilisation of their high tensile strength. Similarly, their hollow sections are prone to compression (bending) buckling failure [4, 5], web-flange junction failure in the compression zone [6, 7] and local buckling of walls due to in-plane compression [8-10]. These limitations of pultruded GFRP sections should, therefore, be addressed for their wide acceptance and use in civil engineering applications.

Several researches proposed different geometrical configurations and material combinations to improve the structural performance of hollow pultruded FRP profiles. Hejll et al. [11] experimentally investigated the flexural behaviour of composite beams made by gluing together square GFRP profiles with a layer of carbon FRP bonded to the flanges. They concluded that assembling the profiles together provided a system with a higher stiffness than individual GFRP profiles to satisfy the requirement for a composite bridge. However, the composite beams failed at a strain of around 7500 microstrains, which are only 60% of the strain capacity determined from the coupon tests. They documented that this behaviour mainly resulted from the buckling failure of the top flange of the square pultruded profile. Kumar et al. [12] and Kumar et al. [13] conducted experimental investigations on 76 mm square hollow pultruded GFRP tubes to evaluate their flexural performance. Two, four and eight layered tubes were bonded together using epoxy adhesive and tested under four-point bending test. In the four and eight layered assembly, the layers of FRP tubes glued together such that each layer is perpendicular to the ones above or below it. They mentioned that the proposed combination showed a good flexural performance and met the strength requirement and the other necessary performance criteria of bridge deck applications. However, web-flange junction failure and twisting of the top layer were observed followed by debonding failure between the layers due to the increased number of tubes in the four- and eight-layered beams. In contrast, the two-layered beams exhibited local buckling failure. In another study, Hayes et al. [14] and Schniepp [15] conducted experimental work on pultruded double web beams (DWB) under three- and four-point bending. The beam composed of both E-glass and

carbon fibres in a vunyl ester resin. The beams consistently failed within compression flange at the interface between carbon and glass fibres. Again, the delamination within the compression flange was the final failure mechanism of the DWB. Hayes and Lesko [16] indicated that the relatively thick flange and the free edge effect for these type of composite beams have played a major role in the initiation of the delamination at the interface between the laminates.

Hybrid structural systems wherein GFRP box beam sections were combined with a concrete layer cast onto the top flange and/or a thin layer of carbon fibre bonded to the tension side were developed to prevent the local buckling in the compression flange and delamination failure of the hollow composites sections [17-19]. The addition of stiffer carbon fibres on the bottom flange can further improve the stiffness of the hybrid composite beams. However, most hybrid composite beams failed in a brittle manner due to the failure in the adhesion between the pultruded section and the concrete layer [20]. In order to prevent the adhesion failure, several researchers completely filled the hollow composite sections with concrete instead of just bonding them on top flanges [21-24]. This approach is not optimal for applications governed by pure bending due to tension cracking in the concrete which decreases the concrete core contribution to the bending resistance [25]. Furthermore, this method diminishes the light weight characteristics of FRP profiles. Therefore, several researchers developed hybrid composite beam systems wherein inner GFRP tube is provided to create a void near the tensile zone [22, 26, 27]. The results indicated that the strength and stiffness of the hybrid beams with inner hole are increased compared with those of a totally filled tube. In a recent study on hybrid composite beam where the concrete was reinforced with steel to minimise tensile cracking and a void was introduced towards the tensile zone [25], the behaviour of the composite beam was compared with a conventional RC beam of the same size. The results showed that the flexural strength of the composite beam is 229% higher than that of a conventional RC beam. However, these researches highlighted that failure due to inward buckling, relatively large slippage between concrete and inner steel or GFRP tube are the main factors that affected the flexural behaviour of the tested beams. Additionally, in the applications which required larger beam sizes, the flexural compression strength failure decreases as the beam size increases [28]. Furthermore, the addition weight of the inner tube and the bond between concrete and GFRP remain critical issues in this combination.

The abovementioned previous studies highlighted the following points: (i) effectiveness of GFRP profiles in the construction industry; (ii) instability and failure of hollow beams due to local buckling and delamination of the compression flange; (iii) flexibility in design from assembled pultruded tubes together; (iv) enhancement of strength and serviceability by filling GFRP tubes with concrete; and (v) maintaining the lightweight characteristics of FRP materials by creating voids in the tension zone of infilled concrete. Based on these important characteristics, the concept of assembling pultruded sections together is explored in this study in order to get benefit of the high sectional moment of inertia of the multi-celled section and flexibility in design. This multi-celled beam concept was achieved by gluing together 2, 3, and 4 GFRP sections with 125mm x 125 mm cross section. Moreover, partial filling is introduced by filling only the top cell of the multi-celled beams with concrete having two different compressive strengths to prevent local buckling failure but keeping the weight minimum. An experimental investigation was then conducted to evaluate the flexural behaviour of these beams and comparison was made with the behaviour of their hollow counterparts. The comparison includes the moment and deflection behaviour, ultimate capacity, and failure mechanism. Simplified prediction methods was also proposed to determine the failure load of the hollow and filled multi-celled beams accounting for the combined effect of shear and flexural stresses. The predicted failure load was then compared with the experimental results.

2. Experimental program
2.1. Material properties

The hollow pultruded GFRP square tubes (125 mm x125 mm x 6.5 mm) used in this study are made up of vinyl ester resin and E-glass fibre reinforcement. The tubes consisted of nine plies of $[0^0/+45^0/0^0/-45^0/0^0/-45^0/0^0/+45^0/0^0]$ E- glass fiber manufactured using pultrusion process by Wagner's Composite Fibre Technologies (WCFT), Australia. Tensile and compressive strength properties along the longitudinal direction were evaluated by testing coupon specimens following ASTM D 695 [29] and ISO 527-2 [30] standards and are reported in Table 1. On the other hand, the elastic modulus and shear modulus were determined from tests of the whole section in a previous study by the authors [31]. The burnout test conducted as per ISO 1172 standard [32] revealed that the density and the fibre volume fraction are 2050 kg/m^3 and 78% by weight, respectively. Two types of concrete were used to fill the beams, i.e. Bastion premix concrete and cement grout.

Table 1. Properties of the pultruded GFRP profiles.

2.2. Sample preparation

Fig. 1 shows the preparation of specimens wherein the square pultruded section represents the main component of the multi-cell beams. Prior to bonding, the surfaces of the square sections to be glued were properly ground and cleaned with acetone (Fig. 1a). GFRP profiles were then assembled and bonded together in 2, 3, 4 cells using the BPE® Lim 465 epoxy adhesives (Fig. 1b). Approximately 1 mm thick bond line was applied (Fig. 1c). The bonded sections were then clamped (hand tight) to provide the necessary bond pressure during adhesive curing (Fig. 1d). The excess adhesives were removed from the sides of the bonded beams. After that, the beams were left to harden for 5 days at ambient temperature.

Fig.2 shows the filling process of the pultruded beams with concrete. The beams were fixed in a vertical position prior to casting. The concrete was prepared and mixed for 10 minutes and then poured into the beams. Five concrete cylinders were sampled from each batch for strength testing and cured under the same conditions as the beam specimens. The 28 day average compressive strength for the Bastion premix concrete and the cement grout were 15 and 32 MPa, respectively. The reason for using two types of concrete infill is to investigate their strength effect on the behaviour of the filled beams. After filling, the specimens were cured for 28 days at ambient temperature before they were tested. Prior to the test, plastic square inserts were used for the hollow and filled beams at the loading and support points to prevent any indentation and/or crushing failure at those points and to allow the beam to fail at the location of the maximum and constant bending moment as shown in Fig. 3a.

2.3. Specimen details

The details of the tested beams are given in Table 2. In the table, the specimens were identified by codes. The specimen length depends on the total depth of the beam to maintain the shear span to depth ratio (a/d) at 4.2. The beams were then divided into three groups according to the section configurations as hollow (H), filled with low strength concrete (H-15) and filled with cement grout (H-32). In the identifications 1C, 2C, 3C and 4C, the first number represents the number of cells and the letter C indicates that they are bonded cells. Two beams were tested for each combination.

Figure 1. Preparation process of pultruded sections assembly

Figure 2. Filling process of the pultruded beams with concrete

a) Plastic inserts   b) Steel angles and steel chains

Figure 3. Supporting procedure of the tested beams

Table 2. Descriptions of the pultruded GFRP tested beams.

2.4. Test setup and experimental procedure

A static four – point bending test of the pultruded beams (Fig.4) was performed following the ASTM D7250 [33] standards. The load was applied at two points with a load span of 300 mm. A 2000 kN universal testing machine was used for applying the load at a rate of 3 mm/min. A laser displacement transducer was used to measure the mid span deflection. Additional steel angles and steel chains were used at the supports to avoid any rotation or lateral buckling (Fig. 3b). Uni–axial strain gauges (type PFL-20-11-1L-120) were used to measure the strain at the top and bottom faces of the beams. The applied load and the displacement were measured and recorded using a data logger System 5000. All specimens were tested up to failure to observe the failure mechanisms of the beams.

Figure 4. Flexural test set-up for single and multi-cell beams

3. Experimental results and observations
3.1. Flexural behaviour

The test results of the flexural behaviour of single and multi-cell GFRP pultruded beams under four-point bending are given in Table 3. Failure of hollow beams was identified as a compressive buckling of the top flange at the constant moment region, while the filled sections failed due to the initiation of compression failure on the top fibres of the section. The failure moment was calculated for each beam based on the failure load and the shear span. Top and bottom failure strains are corresponding to the failure loads. The mode of failure for each specimen is also shown in Table 3.

The table shows that the failure moment increased by 105%, 63%, 58% and 38% for 1, 2, 3 and 4 cells beams filled with 32 MPa infill, respectively, compared with hollow specimen. Single cell specimen filled with 32 MPa compressive strength concrete exhibited approximately 14% higher failure moment than specimen filled with 15 MPa compressive strength concrete. A similar behaviour was observed in specimens with 2, 3, 4 bonded cells and the top cell filled with concrete. The results also showed that single and multi-cell filled sections failed with almost similar compression strains regardless of the strength of the infill

6

concrete. However, the failure compression strains values vary depending on the number of bonded specimens. The filled beams failed at approximately 65, 41, 40 and 18 % higher strains than the hollow beams for the specimens' 1C-H, 2C-H, 3C-H and 4C-H, respectively. The main reason of this variation is the relationship between the depth of the specimens and the distance between the applied loads. When the number of bonded cells is increased, the stress concentration increased with a constant loading distance. As a result, the section behaves in a same manner like three point bending moment.

Table 3. Summary of the experimental test results for pultruded GFRP beams.

3.2. Failure mode

The experimental investigations showed that flexural compression failure was the dominant failure mode of all the tested beams in this study. Fig. 5 shows the failure mode of the beams of 1, 2, 3 and 4 bonded cells with hollow and filled configurations. The failure mode of hollow sections initiates due to the local buckling (LB) of the thin walls which eventually result in material degradation and total failure of the beam. The failure occurred under one of the point load and varied cracks appeared on the top surface of the top cell of the section. The cracks developed perpendicular to the longitudinal axis of the section and then progressed to the web-flange junction due to the effect of buckling and finally these cracks propagated into the web, leading to the final failure of the specimens. Fig. 5 a, c and e shows the failure mode of 1C-H-0, 2C-H-0 and 3C-H-0, respectively. It is of interest to mention that no damage was observed in the second and third cells. In addition, there was no delamination or slipping occurred on the glue line. These results suggest that an efficient glue joint was achieved between the pultruded sections, which was provided by the structural epoxy adhesive used.

Figs. 5 b, d and f show the failure mode of the filled specimens 1C-H-32, 2C-H-32 and 3C-H-32, respectively. It can be seen from the figure that the failure of the filled beams was similar to that of hollow beams. However, those beams failed at higher moment due to the contribution of the concrete core. Furthermore, the presence of the concrete core, however, prevented the local buckling of the compression flange which resulted in higher failure strain compared with the hollow beams. Again, the failure started at the compression flange with fibre damage, matrix cracking and delamination. The failure then progressed into the web due to the progress of the flexural cracks with the application of the load and the failure of the concrete core. In contrast, the four bonded cell section showed different mode of failure as shown in Fig. 5 g. The specimen 4C-H-32 failed due to delamination and fibre cracks at the

top flange, web fibre cracks, flange- web junction failure of the second cell and de-bonding between the top and second cell. This type of failure might occur due to the high bearing load level applied to the section. Furthermore, the top filled cell played an important role by applying bearing pressure on the second top cell which results in high level of inter-laminar shear at the flange-web junction. It is interesting to see that the failure of the multi-cell sections was due to top cell failure which did not result in a total collapse of the beam. This behaviour might be considered to be appropriate for structural engineering designs, as the failure was not really catastrophic.

Crack pattern of the concrete core was examined by removing the pultruded GFRP section after failure. Fig. 6 shows the flexural cracks of the specimens filled with concrete (15 MPa) and cement grout (32 MPa). It can clearly be seen from the figure that flexural cracks developed at the bottom of the beam between the loading points. Furthermore, the cracks spread up to the depth of the concrete infill for single section and the bonded sections. 1C-H-32, 2C-H-32 and 3C-H-32 beams showed distinct flexural cracks as shown in Fig. 6 b, d, f and g while 1C-H-15, 2C-H-15 and 3C-H-15 beams showed fine cracks (Fig. 6 a, c and e). This behaviour might be attributed to the brittleness of cement grout which increases with increasing compressive strength. Therefore, different crack patterns were observed. Fig.6 also shows a slight difference between the number of cracks and the cracking area of single cell specimens compared with double and triple cell specimens. These differences are related to the core contribution in the compression zone. On the other hand, similar crack patterns were observed for 4C-H-32 specimen compared with 1C-H-32 specimen due to the effect of de-bonding failure between the layers of the 4 cells beam which increased the deflection of the top cell. It is interesting to note that crushing did not occur for the concrete core at the maximum moment zone although the complete failure occurred at a strain much higher than the ultimate concrete compression strain (Fig. 6). These results indicate that there is a partial confinement effect of the GFRP tube to the concrete core which in turn kept the concrete under compression intact until failure of the tube.

Figure 5. Failure modes of hollow and filled pultruded GFRP beam

Figure 6. Crack patterns at failure of the tested beams

8

4. Analysis and discussion

The effect of different parameters investigated on the flexural behaviour of multi-celled GFRP beams are analysed and discussed in this section.

4.1. Effect of number of cells
4.1.1. Hollow sections

The effect of the number of cells on flexural strength was evaluated by the maximum bending stress experienced by the GFRP beams using the below equation:

$$bending\ stress = \frac{M_b c}{I} \tag{1}$$

where M_b is the bending moment, c is the distance from the neutral axis to the outer top fibre and I is the moment of inertia of hollow section. The relationship of the bending stress and the number of cells is shown in Fig. 7. It can be seen that the single cell pultruded beam failed at a bending stress of 227 MPa. This result represents approximately 41% of the design capacity of the section based on coupon test results. By gluing the pultruded sections together in 2, 3 and 4 cells resulted in higher level of bending stress at failure compared to single cells. Beams with 2, 3, and 4 bonded cells failed at stresses of 280, 254, and 237 MPa, respectively. These stress values are 43%, 46% and 51% of the design capacities of the section based on coupon test results, respectively. The better performance of multi-cell than single cell can be attributed to the better stability provided by the flanges in the glue lines. However, the beam with 2 cells performed better than 3 and 4 cells. This could be due to the higher level of load needed to fail the 3 and 4 cells than 2 cells as shown in Table 3. As the area under the loading point resisting the applied load is the same for all the beams, the beams with 3 and 4 cells are subjected to a higher level of bearing stress at the loading point which increases the tendency of micro-cracks formation in this zone. The same behaviour was observed by [34] and [35] wherein they indicated that the failure strain and failure stress decrease as the beam depth increases due to the micro-cracks concentration at the failure zone. Therefore, the failure of the beam is directly related to the compressive strength of the beam under the vertical loads.

9

The effective flexural stiffness, *EI* of the single and multi-cell beams was also evaluated based on the slope of the linear elastic portion of the load and mid-span deflection curve using the relation:

$$EI_{eff} = \frac{L^2 a}{48} \left(3 - \frac{4a^2}{L^2}\right) \left(\frac{\Delta P}{\Delta v}\right)$$

(2)

where *P* is the total applied load, *L* denotes the span length, *a* is the shear span, $(\Delta P / \Delta v)$ is the slope of the load-deflection curve, EI_{eff} is the effective flexural stiffness. The apparent stiffness modulus, E_{app} of the tested beams was then computed by dividing EI_{eff} by the second moment of inertia *I* of the hollow beam sections. Fig. 8 shows the relationship between the apparent modulus and the number of cells. The results show that the E_{app} of the single cell section is almost equal to that of the bonded cell beams. This behaviour clearly shows that the apparent stiffness is not affected by the number of bonded cells indicating that the contribution of the shear deformation to the total deflection is similar as a result of using same shear span to depth ratio (a/d = 4.2) for all the tested beams. In another study, Muttashar et al. [31] found that shear deformation contributes approximately 30% to the total deflection of beams with a/d=4. Another possible reason for this behaviour is the failure of single and multi-cell beams is almost similar due to the effect of local buckling. These results suggest that the multi-cell sections will provide stronger beams while maintaining the same effective modulus compared with single cell. However, it is noteworthy that the failure stress values of the hollow single and multi-cell specimens represent approximately only 50% of the stress level determined from coupon test due to the fact that the failure is controlled by the local buckling failure of the compression.

Figure 7. Bending strength for the bonded pultruded GFRP sections

Figure 8. Apparent stiffness modulus for the bonded pultruded GFRP beams.

4.1.2. Partially filled concrete beams

Fig. 7 shows the maximum bending stress of the single and multi-cell GFRP beams with 32 MPa compressive strength concrete infill. The maximum bending stress was calculated using equation 1. The figure shows that single cell specimens filled with concrete exhibited 105% higher strength than hollow specimens. This is attributed to the contribution of the concrete core to reduce the local deformation and improve the strength of the section. Similarly filling

the top cell of beams with 2, 3, and 4 cells improved the flexural strength by 63, 57, and 38%, respectively, compared to their hollow counterparts which reflects the positive effect of concrete infill in preventing local buckling failure. However, the effectiveness of the concrete infill decreases with increasing cell numbers. These observations can be explained by the following. First, the flexural strength of the beams is governed more by the GFRP sections and less by the concrete infill. For all GFRP beams tested, failure occurred in a brittle manner due to compression failure of the topmost compression fibre near the loading point. With increasing number of cells, the effect of concrete filling on the bending strength becomes lower due to the higher level of load needed to fail beams compared with single cells which results in high stress concentration between the loading points. The authors believe that the percentage of improvement of the flexural strength becomes higher if the stress concentration is minimised.

Fig. 8 also illustrates the effect of concrete infill on the apparent stiffness modulus E_{app} of single and multi-cell specimens. Firstly, the effective flexural stiffness EI_{eff} was calculated based on the slope of the linear elastic portion of the load and mid-span deflection after tensile cracking using equation 2 then the I of the hollow sections has been used to calculate E_{app} It is found that the concrete infill has a noticeable effect on the apparent modulus for single and multi-cell beams. It can be seen from the figure that the E_{app} of the single cell specimens increased by 22% compare to hollow specimens while the beams with 2, 3 and 4 cells improved by 18, 17 and 10 %, respectively over their counterpart hollow specimens.

The failure behaviour also changes by filling the top GFRP section with concrete as shown in Fig 5. It improved its flexural stiffness to some extent. The deformation of the infilled beams increases with the increase in the external load. This deformation becomes higher for 2, 3 and 4 cells section due to the increase in the applied load. Furthermore, the infilled beams show high deflection which means high curvature. Due to the effect of shear span to depth ratio in addition to high deflection, maximum compressive stresses is located at the top section along the longitudinal direction of the beam and compressive stresses was also developed in the shear span along the line connecting load and support. Theses stresses might result in high compressive stress near the load point due to the effect of local stress concentration. Consequently, the effect of concrete infill tends to be less for beams with higher cell numbers in the cross section. In addition, it is obvious that the total stiffness of the composite sections is a combination of those of their components. However, due to tensile cracking of concrete and the increase of the number of bonded cells, lower contribution of the concrete infill was

achieved. On the other hand, even though the improvement in the flexural stiffness decreases with increased number of cells, these percentages represent the improvement in the flexural stiffness from the overall stiffness of each section. That means 10% increase in the overall stiffness of 4 cell beams is more effective than the 22% increase for single cell beams as only 25% of the section is filled while 100% is filled for the single section. The experimental results suggested that, in the construction of multi-cell pultruded beams, filling the top cell with concrete will result in stronger and stiffer beam than the hollow beams.

4.2. Effect of concrete compressive strength

Fig. 9 shows the influence of concrete compressive strength on the flexural strength of beams with 1, 2 and 3 cells. The beams filled with 32 MPa compressive strength exhibited higher flexural strength than beams filled with 15 MPa by 16, 13 and 10 % for 1, 2 and 3 cells, respectively. These percentages are minimal compared to the increase in concrete compressive strength from 15 MPa to 32 MPa. The possible reason for the limited increase in the flexural strength is that the failure of those sections is governed by the compression failure of the pultruded profiles. In addition, the difference in the neutral axis location might be another reason for this variation. Concrete of low strength shows higher neutral axis depth which results in higher contribution in the calculation of the flexural strength.   However, single specimen shows higher strength gain compared with other specimens due to the difference in the failure mode between single and multi-cells sections.

Fig. 10 shows the influence of concrete compressive strength on the flexural stiffness of the 1, 2 and 3 cell beams. The flexural stiffness, *EI* was also evaluated based on the slope of the linear elastic portion of the load and mid-span deflection curve after concrete cracking using equation 2. The figure indicates that the flexural stiffness of the beams filled with 15 MPa compressive strength concrete is almost similar to those beams filled with 32 MPa concrete. It is seen that 1, 2 and 3 cells specimens filled with 32 MPa concrete are only 2.2, 1.2, and 0.4 % stiffer, respectively, than beams filled with 15 MPa concrete. Two possible reasons may explain this behaviour. Firstly, it is clear from the experimental results that the overall behaviour of the tested beams is governed by the GFRP profile's mode of failure due to the fact the failure occurred at a very high strain level compared with strain failure of concrete. Secondly, due to the difference in modulus of elasticity between the two concrete types and after the occurrence of tensile cracks, higher area of low strength concrete infill is required to

12

maintain the equilibrium in the internal forces compared with higher strength concrete. Consequently, the concrete compressive strength shows a limited effect on the flexural capacity. On the other hand, although the concrete core is located in the compression zone for beams of 3 cells or more, the mode of failure is slightly different from that of beams of 1 and 2 cells. Figs.s 5 and 6 show that the concrete core cracked and local buckling failure happened in the cell located under the filled cell. This behaviour explains the limited contribution of the concrete core on the stiffness. It can be concluded that the flexural behaviour of the tested specimens in this study was not significantly affected by the increase in the compressive strength.

Figure 9. Effect of concrete compressive strength on the moment capacity of the beams with 1, 2 and 3 cells

Figure 10. Effect of concrete compressive strength on the flexural stiffness of the 1, 2 and 3 cells pultruded GFRP sections

5. Theoretical analysis and evaluation
5.1. Failure load prediction

The observed failure mode of hollow beams was local buckling of the compression flange under the loading points in addition to a shear crack in the shear span (Fig. 5). At the location of loading, the maximum bending moment and shear forces exist. Manalo [36] and Awad et al. [37] highlighted that for composite beams with a shear span-to-depth ratio (a/d) less than 4.5, failure will occur due to a combined effect of shear and flexural stress. In the current study, the tested beams have an a/d = 4.2. Similarly, Bank [1] stated that, when the beam is subjected to high shear force and bending moment, the web will experience a combination of shear stress (τ) and flexural (compressive or tensile) stress ($\square$). Under this condition, the failure of the multi-celled composite beams is expected to occur when the sum of the ratios of the actual shear and flexural stresses to that of the allowable stresses approaches unity as given by:

$$\frac{\sigma_{act}}{\sigma_{all}} + \frac{\tau_{act}}{\tau_{all}} \leq 1 \qquad\qquad (3)$$

where σ_{act} is the actual flexural compressive stress carried by the topmost fibre of the GFRP tube calculated as:

$$\sigma_{act} = \frac{Mc}{I} = \frac{Pac}{2I} \qquad\qquad (4)$$

where P is the applied load, a is the shear span, c is the distance from the neutral axis of the section to the topmost fibre, and I is the second moment of inertia of the section. On the other hand, the actual shear stress τ_{act} can be determined using the below equation:

$$\tau_{act} = \frac{VQ}{It} = \frac{PQ}{2It} \qquad\qquad (5)$$

where V represents the shear force ($P/2$), Q is the first moment of area, and t is the total thickness of the section. As the elastic instability of the pultruded GFRP sections in compression is governed by the local buckling [38], Muttashar et al. [31] suggested to use buckling stresses, σ_{cr}^{local} instead of the allowable compressive stresses in equation 3. An approximate expression to determine the buckling stresses for free and rotationally restrained orthotropic plates has been proposed by Kollár [39]. In this method, the local buckling stress of the section is calculated by considering the web and flange to be separate from each other and assuming them as orthotropic plates subjected to uniaxial compression and elastically restrained along their common edge. This buckling stress equation is given below:

$$\sigma_{cr}^{local} = min\left[\sigma_{loc,f}, \sigma_{loc,w}\right] \qquad\qquad (6)$$

where $\sigma_{loc,f}$ and $\sigma_{loc,w}$ are the critical normal stresses of flanges and webs, respectively. The critical normal stresses of the flanges and the webs can then be written as [39].

$$\sigma_{loc,f} = \frac{\pi^2}{b_f^2 t_f} ¿ \frac{(D_L D_T)(¿\xi) + (D_< + 2D_S)(2 + 0.62\xi_{box-flange}^2)}{2\sqrt{¿}} \qquad (7)$$

$$\sigma_{loc,w} = \frac{\pi^2}{d_w^2 t_w}\left[13.9\sqrt{(D_L D_T)} + 11.1 D_< + 22.2 D_S\right] \qquad\qquad (8)$$

The compression flange will buckle before one of the webs if $\left(\sigma_{ss}^{ss}\right)_f / \left(E_L\right)_f < \left(\sigma_{ss}^{ss}\right)_w / \left(E_L\right)_w$. In this case, the web restrains the rotation of the flanges and the spring constant is given as:

14

$$k_{box-flange} = \frac{4(D_T)_w}{d_w}\left[1 - \frac{(\sigma_{ss}^{ss})_f (E_L)_w}{(\sigma_{ss}^{ss})_w (E_L)_f}\right] \qquad (9)$$

where

$$(\sigma_{ss}^{ss})_f = \frac{2\pi^2}{b_f^2 t_f}\left(\sqrt{(D_L D_T)} + D_< + 2 D_S\right) \qquad (10)$$

$$(\sigma_{ss}^{ss})_w = \frac{2\pi^2}{d_w^2 t_w}\left(13.9\sqrt{(D_L D_T)} + 11.1 D_< + 22.2 D_S\right) \qquad (11)$$

$$\xi_{box-flange} = \frac{1}{1 + 10\left[(D_T)_f / k_{box-flange} b_f\right]} \qquad (12)$$

$$D_L = \frac{E_L^c t_f^3}{12(1 - v_L v_T)} \qquad (13)$$

$$D_T = \frac{E_T^c}{E_L^c} D_L \qquad (14)$$

$$D_< = v_T D_L \qquad (15)$$

$$D_s = \frac{G_< t_f^3}{12} \qquad (16)$$

$$v_T = \frac{E_T^c}{E_L^c} v_L \qquad (17)$$

where b_f and t_f are the width and thickness of the flange, respectively, d_w and t_w are the depth and thickness of the web, respectively, E_T^c is longitudinal compression modulus, E_L^c is transverse compression modulus, $G_<$ is the in-plane shear modulus, and v_L, v_T are the major (longitudinal) and minor (transverse) Poisson ratios, respectively. On the other hand, the web buckles first when $(\sigma_{ss}^{ss})_f / (E_L)_f > (\sigma_{ss}^{ss})_w / (E_L)_w$. In this case, Kollár [39] suggested to take K= 0 as a conservative estimate.

In terms of the shear stress, the web of the GFRP tube is highly susceptible to buckle in location of high shear forces while flange buckling which typically occurs under the loading

point or near the supports. The critical shear buckling stress of an orthotropic web can be determined using the relation (18) proposed by [40]:

$$\tau_{cr}^{local} = \frac{4\,k_{<}\sqrt[4]{D_L\,D_T^3}}{d_w^2\,t_w} \qquad (18)$$

where

$$k_{<} = 8.125 + 5.045\,K \qquad \text{for K} \le 1 \qquad (19)$$

and
$$K = \frac{2\,D_s + D_{<}}{\sqrt{D_L\,D_T}} \qquad (20)$$

For the infilled section, the flexural buckling stress (σ_{cr}^{local}) is different. Wright [41] highlighted that the infill concrete will contribute in delaying or eliminating the local buckling in the compression flange. However, it has a minimum effect on the buckling of the webs due to the insufficient connection between the tube and the concrete. As a result, the section will develop more resistance to the applied load and will reach its maximum allowable compressive stress (Table 1). Under such condition, equation 3 can be used to predict the failure of 1, 2 and 3 cells sections but with considering τ_{cr}^{local} as the effective shear stress instead of τ_{all}. With these assumptions, the predicted failure load, P_H of single and multi-celled hollow beams is given by equation 21 while the predicted failure load, P_F of their counterpart filled beams is given by equation 22.

$$P_H = \frac{1}{\dfrac{ac}{2\,I\,\sigma_{cr}^{local}} + \dfrac{Q}{2\,It\,\tau_{cr}^{local}}} \qquad (21)$$

$$P_F = \frac{1}{\dfrac{ac}{2\,I\,\sigma_{all}} + \dfrac{Q}{2\,It\,\tau_{cr}^{local}}} \qquad (22)$$

5.2. Predicted results and comparison with the experiments

Table 4 summarises the predicted failure load for single and multi-cell beams with and without concrete infill. The percentage difference between the experimental and predicted failure loads is also given in Table 4. It is clear that the predicted failure load using combined effect of shear and flexural stresses given in Eq. 21 showed a very good agreement with the

16

experimental results for single and multi-celled hollow beams. The equation over predicts the failure load by only 4.5% for single cell section. In addition, the equation overestimate the failure load for 2,3 and 4 cells section by only 3.3%, 0.5% and 1.1%, respectively. On the other hand, the predicted failure load in Eq. 22 is only 2.7% higher compared to the experimental failure load for 1, 2 and 3 cells filled beams, respectively. However, for the filled beam with 4 cells, Eq. 22 overestimated the predicted failure load by 8%. This relatively high difference between the predicted and the actual failure load can be due to the complex state of stress under the loading point for the infilled beams with 4 cells. It is noted from Fig. 5g that the beam with 4 cells exhibited a bearing failure by flange-web junction separation of the second top cell. This failure is due to the high inter-laminar stress at the flange-web junction which has exceeded the shear capacity limit of the pultruded section. Wu and Bai [42] indicated that pultruded FRP beams subject to concentrated loads in the plane of the web are more likely to show inter-laminar shear failure due to bearing stresses at the web-flange junction. They then proposed an equation to estimate the nominal web crippling capacity of the pultruded GFRP beams:

$$R_N = f_s \, x \, A_{shear}$$ (23)

where

$$A_{shear} = 2 \, x \, t_w \, x \, b_{plate}$$ (24)

and b_{plate} represents the width of the bearing plate and f_s is the inter-laminar shear strength of the section. Using this equation, the failure load of the filled beam sections was calculated and presented in Table 4. Comparison between the predicted and actual failure load showed only a 6.1% difference. The difference between the predicted and the measured failure load is probably due to the slightly higher actual sheared area. Thus, it can be concluded that the failure load of 1, 2 and 3 cells filled beams can be accurately predicted using linear combination of shear and flexural stresses while the bearing stress formula gives a better prediction of the failure load for the filled beam with 4 cells.

Table 4. Predicted failure load and difference with the experimental failure load.

6. Conclusions

This study presented the results of four point bending tests on hybrid multi-cell hollow and concrete filled GFRP tubes. The main parameters examined in this study are number of cells, cell configuration and compressive strength of concrete core. A simple theoretical model was

17

implemented and used to predict the flexural behaviour of multi-celled GFRP beams. Based on the results, the following conclusions can be drawn:

- Multi-cell hollow beams show better flexural performance than single cell. The single cell beams failed with 40% of its design capacity based on coupon tests while the failure of the multi-cell beams reached 51%. Although, there is an improvement in the failure stress levels for multi-cell beams, these levels are still lower than the stress level determined from coupon test due to the fact that the failure is controlled by the local buckling of the compression.

- The failure of the multi-cell sections was due to the compression failure in the top cell which did not result in a total collapse of the beam. This behaviour might be considered to be appropriate for structural engineering designs, as the failure was not really catastrophic.

- The flexural strength of beams filled with concrete at the topmost section is 105%, 63%, 57% and 38% for 1, 2, 3 and 4 cell sections, respectively, higher than that of hollow section. This reflects the positive effect of concrete infill in preventing local buckling failure.

- Compression flange failure associated with fibre breakage, matrix cracking and delamination was the main mode of failure of the filled beams. The failure then progressed into the webs with increasing applied load due to the effect of flexural cracks in the concrete core.

- Concrete infill has a noticeable effect on the apparent modulus for single and multi-cell beams. The E_{app} increased by as much as 22% compared to the hollow beam section.

- Beams filled with 32 MPa compressive strength exhibited 14% higher flexural strength than beams filled with 15 MPa. However, increasing the compressive strength from 15 to 32 MPa has a minimal effect on the flexural stiffness of the filled beams due to the fact that the behaviour of the tested beams controlled by the behaviour of GFRP tubes.

- The combined effect of shear and flexural stresses should be considered to reliably predict the failure load of hollow and filled multi-celled beams but with some modifications. Using the buckling stresses in bending and shear instead of the

allowable stresses gives a reliable estimation of the failure load for hollow sections while using the allowable compressive stress and critical shear stress is accurate for the filled section.

- The failure of filled beams with 4 cells is governed by inter-laminar shear failure at the web-flange junction and the failure load can be estimated reasonably well by calculating the nominal web crippling capacity of the pultruded GFRP beam.

Acknowledgement

References

[1] Bank LC. Application of FRP Composites to Bridges in the USA. Japan Society of Civil Engineers (JSCE), Proceedings of the International Colloquium on Application of FRP to Bridges, January 202006. p. 9-16.
[2] Ryall M, Stephenson R. Britannia bridge: from concept to construction. Proceedings of the ICE-Civil Engineering: Thomas Telford; 1999. p. 132-43.
[3] Gand AK, Chan T-M, Mottram JT. Civil and structural engineering applications, recent trends, research and developments on pultruded fiber reinforced polymer closed sections: a review. Frontiers of Structural and Civil Engineering. 2013;7:227-44.
[4] Mottram J. Lateral-torsional buckling of a pultruded I-beam. Composites. 1992;23:81-92.
[5] Davalos JF, Qiao P. Analytical and experimental study of lateral and distortional buckling of FRP wide-flange beams. Journal of Composites for Construction. 1997;1:150-9.
[6] Bai Y, Keller T, Wu C. Pre-buckling and post-buckling failure at web-flange junction of pultruded GFRP beams. Materials and structures. 2013;46:1143-54.
[7] Turvey GJ, Zhang Y. Shear failure strength of web–flange junctions in pultruded GRP WF profiles. Construction and Building Materials. 2006;20:81-9.
[8] Bank LC, Nadipelli M, Gentry TR. Local buckling and failure of pultruded fiber-reinforced plastic beams. Journal of engineering materials and technology. 1994;116:233-7.
[9] Barbero EJ, Fu S-H, Raftoyiannis I. Ultimate bending strength of composite beams. Journal of Materials in Civil Engineering. 1991;3:292-306.
[10] Hai ND, Mutsuyoshi H, Asamoto S, Matsui T. Structural behavior of hybrid FRP composite I-beam. Construction and Building Materials. 2010;24:956-69.
[11] Hejll A, Täljsten B, Motavalli M. Large scale hybrid FRP composite girders for use in bridge structures—theory, test and field application. Composites Part B: Engineering. 2005;36:573-85.
[12] Kumar P, Chandrashekhara K, Nanni A. Testing and evaluation of components for a composite bridge deck. Journal of reinforced plastics and composites. 2003;22:441-61.
[13] Kumar P, Chandrashekhara K, Nanni A. Structural performance of a FRP bridge deck. Construction and Building Materials. 2004;18:35-47.
[14] Hayes M, Lesko J, Haramis J, Cousins T, Gomez J, Masarelli P. Laboratory and field testing of composite bridge superstructure. Journal of Composites for Construction. 2000.
[15] Schniepp TJ. Design manual development for a hybrid, FRP double-web beam and characterization of shear stiffness in FRP composite beams. 2002.
[16] Hayes MD, Lesko JJ. Failure analysis of a hybrid composite structural beam. Composites Part A: Applied Science and Manufacturing. 2007;38:691-8.
[17] Triantafillou T, Meier U. Innovative design of FRP combined with concrete. Advanced Composite Materials in Bridge and Structures. 1992:491-9.
[18] Canning L, Hollaway L, Thorne A. Manufacture, testing and numerical analysis of an innovative polymer composite/concrete structural unit. Proceedings of the ICE-Structures and Buildings. 1999;134:231-41.

[19] Van Erp G, Heldt T, Cattell C, Marsh R. A new approach to fibre composite bridge structures. Proceedings of the 17th Australasian conference on the mechanics of structures and materials, ACMSM17, Australia2002. p. 37-45.

[20] Chakrabortty A, Khennane A, Kayali O, Morozov E. Performance of outside filament-wound hybrid FRP-concrete beams. Composites Part B: Engineering. 2011;42:907-15.

[21] Aydin F, Saribiyik M. Investigation of flexural behaviors of hybrid beams formed with GFRP box section and concrete. Construction and Building Materials. 2013;41:563-9.

[22] Fam AZ, Rizkalla SH. Flexural behavior of concrete-filled fiber-reinforced polymer circular tubes. Journal of Composites for Construction. 2002;6:123-32.

[23] Gautam BP, Matsumoto T. Shear deformation and interface behaviour of concrete-filled CFRP box beams. Composite Structures. 2009;89:20-7.

[24] Muttashar M, Manalo A, Karunasena W, Lokuge W. Influence of infill concrete strength on the flexural behaviour of pultruded GFRP square beams. Composite Structures. 2016;145:58-67.

[25] Abouzied A, Masmoudi R. Structural performance of new fully and partially concrete-filled rectangular FRP-tube beams. Construction and Building Materials. 2015;101:652-60.

[26] Khennane A. Manufacture and testing of a hybrid beam using a pultruded profile and high strength concrete. Australian Journal of Structural Engineering. 2010;10:145-56.

[27] Idris Y, Ozbakkaloglu T. Flexural behavior of FRP-HSC-steel composite beams. Thin-Walled Structures. 2014;80:207-16.

[28] Kim J-K. Size effect on flexural compressive strength of concrete specimens. 2000.

[29] ASTM D 695. Standard test method for compressive properties of rigid plastics, ASTM International, Philadelphia, USA. 2010.

[30] ISO 527-2. Plastics: Determination of tensile properties. 1996.

[31] Muttashar M, Karunasena W, Manalo A, Lokuge W. Behaviour of hollow pultruded GFRP square beams with different shear span-to-depth ratios. Journal of Composite Materials. 2015:0021998315614993.

[32] ISO 1172. Textile-glass-reinforced plastics, prepegs, moulding compounds and laminates: Determination of the textile-glass and mineral-filler content- Calcination methods. 1996.

[33] ASTM D7250. ASTM D7250/D7250M-06 Standard practice for determine sandwich beam flexural and shear stiffeness. West Conshohocken, (PA): ASTM International; 2006.

[34] Kim J-K, Yi S-T, Kim J-HJ. Effect of specimen sizes on flexural compressive strength of concrete. ACI Structural Journal. 2001;98.

[35] Kim J-K, Yi S-T. Application of size effect to compressive strength of concrete members. Sadhana. 2002;27:467-84.

[36] Manalo A. Behaviour of fibre composite sandwich structures under short and asymmetrical beam shear tests. Composite Structures. 2013;99:339-49.

[37] Awad ZK, Aravinthan T, Manalo A. Geometry effect on the behaviour of single and glue-laminated glass fibre reinforced polymer composite sandwich beams loaded in four-point bending. Materials & Design. 2012;39:93-103.

[38] Tomblin J, Barbero E. Local buckling experiments on FRP columns. Thin-Walled Structures. 1994;18:97-116.

[39] Kollár LP. Local buckling of fiber reinforced plastic composite structural members with open and closed cross sections. Journal of structural engineering. 2003;129:1503-13.

[40] Bank LC. Composite for Construction Structural Design with FRP Materials. New Jersey: Jone Wiley & Sons, 2006.

[41] Wright H. Local stability of filled and encased steel sections. Journal of structural engineering. 1995;121:1382-8.

[42] Wu C, Bai Y. Web crippling behaviour of pultruded glass fibre reinforced polymer sections. Composite Structures. 2014;108:789-800.

Allan Manalo, BScEng, MEng, PhD
Senior Lecturer in Civil Engineering (Structural)
Centre of Excellence in Engineered Fibre Composites
Faculty of Health, Engineering & Sciences
University of Southern Queensland
Toowoomba QLD 4350
Australia

1 July 2016

Professor A. J. M. Ferreira
Editor
Composite Structures
Elsevier

Dear Prof Ferreira:

Please find the attached Word file of "**Flexural Behaviour of Multi-Celled GFRP Composite Beams with Concrete Infill: Experiment and theoretical analysis**" by Majid Muttashar, Allan Manalo, Warna Karunasena, and Weena Lokuge. We would like to have this manuscript reviewed by the **Composite Structures** for possible publication. We guarantee that the contribution is an original material, has not been published previously and is not under consideration for publication elsewhere. All the materials and information contained in the paper are not restricted and are available to all.

Should you need to contact me, please use the above address or call me at (+61) 7 4631 2547. You may also contact me by fax at (+61) 7 4631 2110 or via email at manalo@usq.edu.au.

Sincerely,
Allan Manalo

All Figures

Figure 1. Preparation process of pultruded sections assembly.

Figure 2. Filling process of the pultruded beams with concrete.
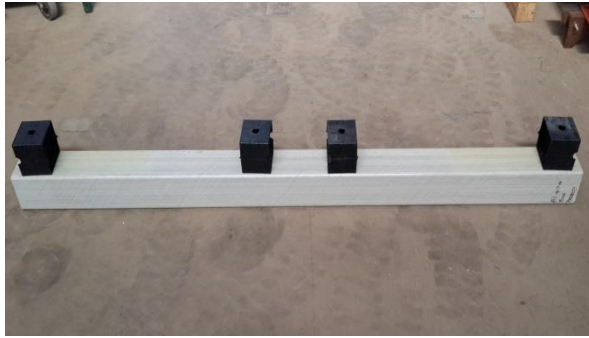
a) Plastic inserts   b) Steel angles and steel chains

Figure 3. Supporting procedure of the tested beams.
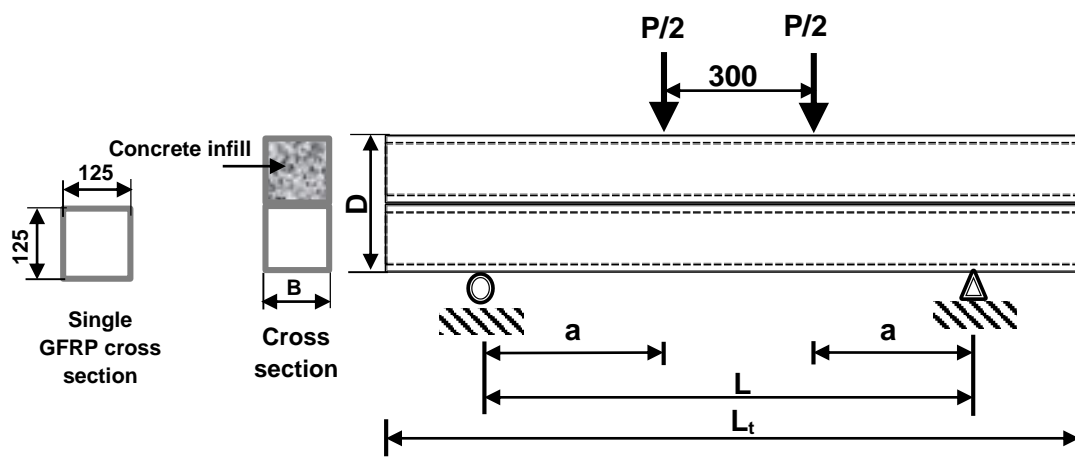
All dimensions are in millimetres

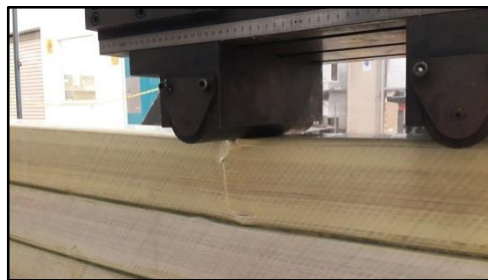**Figure 4.** Flexural test set-up for single and multi-cell beams.
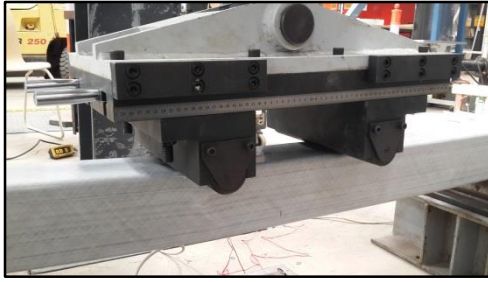
a) 1C-H-0
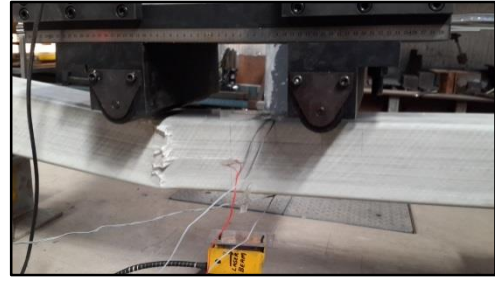
b) 1C-H-32
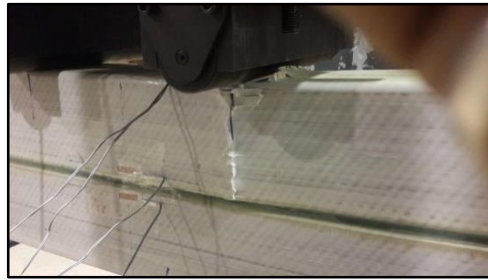
c) 2C-H-0

d) 2C-H-32

e) 3C-H-0

f) 3C-H-32

g) 4C-H-32

Figure 5. Failure modes of hollow and filled pultruded GFRP beam

a) 1C-H-15

b) 1C-H-32

c) 2C-H-15

d) 2C-H-32
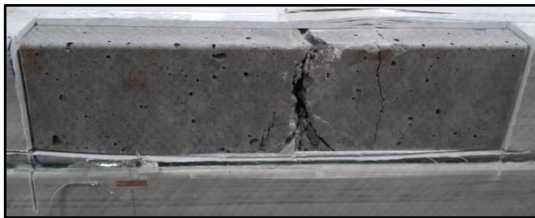
e) 3C-H-15

f) 3C-H-32

g) 4C-H-32

Figure 6. Cracks pattern at failure of the tested beams.
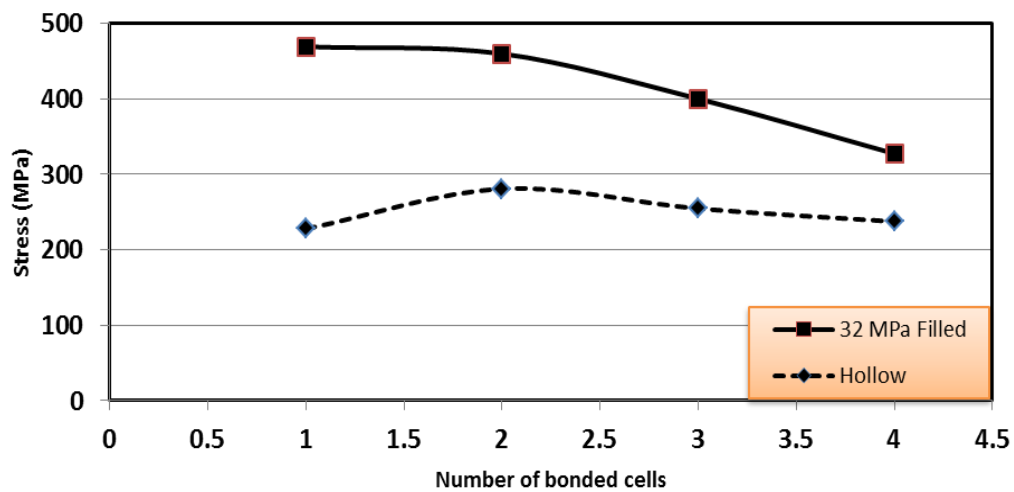
Figure 7. Bending strength for the bonded pultruded GFRP sections.
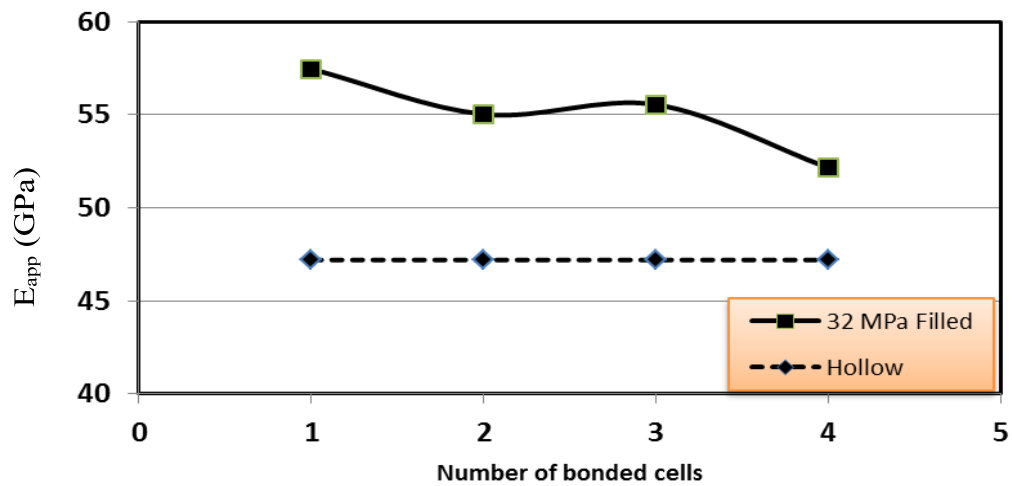
Figure 8. Apparent stiffness modulus for the bonded pultruded GFRP beams.
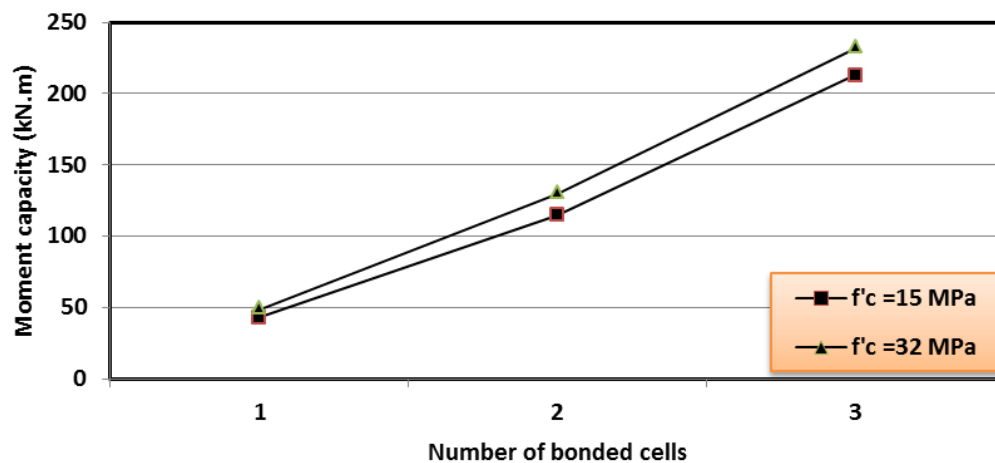
Figure 9. Effect of concrete compressive strength on the moment capacity of the beams with 1, 2 and 3 cells.
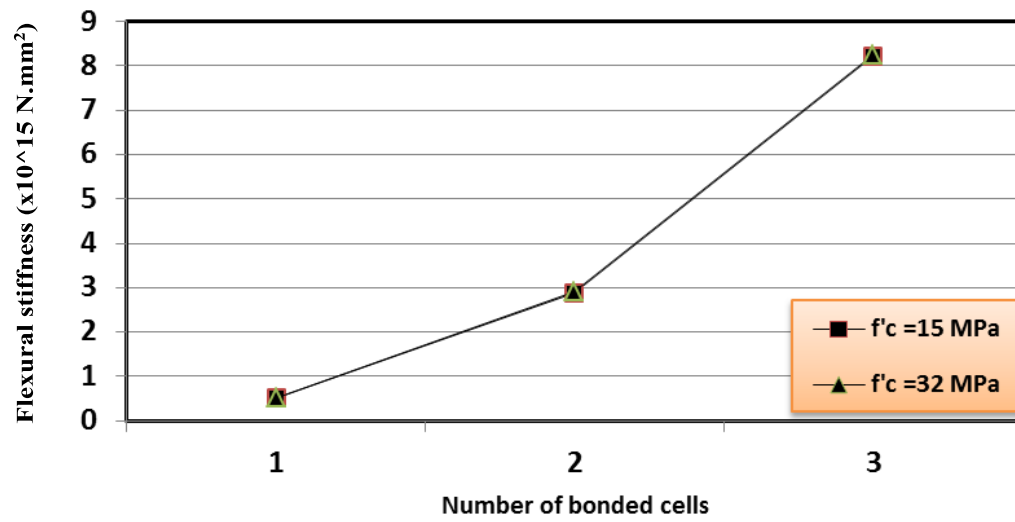
Figure 10. Effect of concrete compressive strength on the flexural stiffness of the 1, 2 and 3 cells pultruded GFRP sections.

All Tables

Table 1. Properties of the pultruded GFRP profiles.

Material property	Symbol	Property value	unit
Density	ρ	2050	kg/m^3
Tensile stress	σ_t	596	MPa
Tensile strain	ε_t	16030	microstrain
Compressive stress	σ_c	550	MPa
Compressive strain	ε_c	11450	microstrain
Inter-laminar shear	τ	86	MPa
Elastic modulus	E	47.2	GPa
Shear modulus	G	4	GPa

Table 2. Descriptions of the pultruded GFRP tested beams.

Specimen	Illustration	B (mm)	D (mm)	L_t (mm)	L (mm)	a (mm)	f_c' MPa
1C-H-0		125	125	2000	1350	525	-
1C-H-15		125	125	2000	1350	525	15
1C-H-32							32
2C-H-0		125	250	2750	2400	1050	-
2C-H-15		125	250	2750	2400	1050	15
2C-H-32							32
3C-H-0		125	375	3700	3450	1575	-
3C-H-15		125	375	3700	3450	1575	15
3C-H-32							32
4C-H-0		125	500	5000	4500	2100	-
4C-H-32		125	500	5000	4500	2100	32

Table 3. Summary of the experimental test results for pultruded GFRP beams.

Specimen	D	L	a	Failure load	Failure moment	Deflection	Bottom strain	Top strain	Failure mode
	(mm)	(mm)	(mm)	(kN)	(kN.m)	(mm)	μ ε	μ ε	
1C-H-0	125	1350	525	90.6	23.8	18.8	5500	4000	[a] LB
1C-H-15				161.5	43	29.8	9104	8113	[b] CF
1C-H-32				186.6	49	34	10329	8443	CF
2C-H-0	250	2400	1050	151.2	79.4	34.7	6324	4242	LB
2C-H-15				217	114	42.7	7520	6675	CF
2C-H-32				247.6	130	48	8947	7679	CF
3C-H-0	375	3450	1575	187.5	147.6	42.4	5496	3979	LB
3C-H-15				261.6	214	55.8	7331	6928	CF
3C-H-32				294.6	232	60.5	7708	7090	CF
4C-H-0	500	4500	2100	225	236.5	48	5400	4490	LB
4C-H-32				348	365	63.9	6409	5338	CF

[a] LB= Local buckling failure

[b] CF= GFRP material failure at the compression side

Table 4. Predicted failure load and difference with the experimental failure load.

Number of cells	Hollow section			Filled section				
	Exp.	Eq. (21)	% Diff.	Exp.	Eq. (22)	% Diff.	Eq. (23)	% Diff.
1	90.6	95	4.5	186.6	192	2.7	326.5	42.8
2	151	156	3.3	247.6	250	1.3	326.5	24.1
3	187.5	188	0.5	294.6	299	1.7	326.5	9.7
4	243	245	1.1	348	378	8.1	326.5	-6.1